


Research Article

A Trans-Scale Study on the Influence of Water Content and Particle Size on Matric Suction

Cheng Pu ^{1,2}, Fengyin Liu,² Yuetao Li,¹ and Zhaolin Zeng²

¹PowerChina Northwest Engineering Corporation Limited, China

²Xi'an University of Technology, China

Correspondence should be addressed to Cheng Pu; 1909488416@qq.com

Received 30 January 2023; Revised 29 May 2023; Accepted 30 May 2023; Published 14 June 2023

Academic Editor: Mohammed Fattah

Copyright © 2023 Cheng Pu et al. This is an open access article distributed under the Creative Commons Attribution License, which permits unrestricted use, distribution, and reproduction in any medium, provided the original work is properly cited.

Exploring the water retention properties of unsaturated soil from the perspective of a liquid bridge has been a popular issue in recent years. This study first measures the soil–water characteristic curves (SWCCs) of granular specimens to determine the influence of particle size on matric suction from a macroscopic perspective. Then, the internal mechanism of the influence of particle size and volumetric water content on matric suction is analyzed from the mesoscopic perspective by using the Young–Laplace (Y–L) equation to calculate matric suction between two equal spheres. The macroscopic and mesoscopic experiments both show that matric suction decreases with an increase in particle radius. Moreover, identifying the internal mechanism of SWCC from the liquid bridge perspective is only applicable when the influence of gravity can be disregarded or is in the transitional stage. The influence of volumetric water content and sphere radius on matric suction is mostly caused by the variation in the outer radius of the liquid bridge (r_1) and the neck radius of the liquid bridge (r_2). With an increase in volumetric water content and sphere diameter, the increasing rate of r_1 is much higher than r_2 , and the macroscopical matric suction gradually decreases.

1. Introduction

Some critical characteristics of unsaturated soil are its water retention properties. A proper understanding of these properties has been a hot issue in scientific research and forms the foundation and basis for geotechnical engineering construction. The study of the water retention properties of unsaturated soil originated in the field of soil science. Researchers have used matric suction to represent the capability to absorb water from the ambient atmosphere of soil and established the soil–water characteristic curve (SWCC) to characterize the relationship between water energy and quantity in soil. During the late 1980s, the concept of SWCC was introduced to the study of unsaturated soil. For a long time, many scholars have used matric suction to represent the water retention properties of unsaturated soil and have achieved considerable progress. A typical SWCC presents an “S” shape, which can be divided into the residual stage at high suction, the transition stage at intermediate suction,

and the boundary effect stage at low suction [1]. The intersection point of the tangent line of the residual stage and the transition stage was defined as the residual water content point, and the intersection point of the tangent line of the transition stage and the boundary effect stage was defined as the air-entry value, where the suction dominates the capillary water forces in the largest pore in the soil [2]. Compaction degree, initial water content, grain size distribution, and stress history all influence SWCC to different extents [3–6].

However, with improved understanding, it was found that the measurement of matric suction under different initial conditions was greatly influenced by external conditions and soil properties. Therefore, it is not enough to correctly understand the inner mechanisms of water retention in unsaturated soil. As a typical bulk material, when soil absorbs water from the ambient atmosphere, a liquid bridge will be formed in the contact area of two soil particles. Thus, some researchers proposed that the variation of water retention properties can be regarded as the development of a

liquid bridge [7], and the investigation of the liquid bridge had been gained increased attention. The pioneering study of the liquid bridge can be traced back to the field of surface science started by Fisher [8], who studied the liquid bridge formed between two equal spheres. Gillespie and Settineri [9] and Clark et al. [10] assumed the profile of liquid to be circular to find a simple and effective numerical computation method. The liquid bridge was divided into four types, such as pendular, funicular, capillary, and slurry, according to the value of saturation and the interaction mode between the liquid bridge and particles, as shown above [11, 12].

In recent years, researchers in the field of geotechnical engineering have actively explored the water retention properties of unsaturated soil from the perspective of the liquid bridge. By using gray processing software to process, the images of unsaturated granular specimens obtained via X-ray microcomputed tomography, solid–water, and water–gas boundaries were identified, and SWCCs were quantified by measuring the value of solid–water and water–gas contact angles [13]. Molenkamp and Nazemi [14] used a dimensionless method to investigate the relationship between liquid force and solid–liquid contact angle, sphere radius, and surface roughness, finding that the dimensionless matric suction increases with the increase of particle radius, and that the cohesion induced by matric suction exists in good grain gradation soil even in a dry environment. Likos and Lu [15] investigated the effect of solid–liquid contact angle on the strength of soil in the dry–wet cycle processes by varying the contact angle from 0° to 40° to simulate the drying-to-wetting processes; the results show that when matric suction equals, the larger the solid–liquid contact angle is, the smaller the volume water content gain. The effect of the capillary force on the intergranular stress during the wetting process is greater than that in the drying process. Considering the contact repulsion, friction, and capillary cohesion between particles, Jiang and Li [16] and Soulié et al. [17] established a contact model that can represent the interaction between particles and liquid bridges to simulate the macroscopic mechanical behavior of unsaturated sand. Simplifying the soil mass as spherical particles aggregate, Yang and Lu [18] established a theoretical model for predicting SWCC in the case of dehydration according to the geometric relationship between particles and the liquid bridge, and the influence of contact angle on the SWCCs was also studied. Different types of liquid bridges corresponded to each stage of SWCC, according to the saturation of the specimen and the liquid state between particles [19, 20].

The residual saturation zone is the zone where water is tightly absorbed into the soil particles [21]. In the transition stage, matric suction decreases with an increase in volumetric water content, a pendular liquid bridge is formed between two spheres, and the geometries of the interparticle pore water menisci dramatically change [22, 23]. With an increase in water content, a liquid bridge may be shared by three particles, and it transforms from being pendular to being funicular [24]. As the water content increases continuously, the SWCC enters the boundary effect section, the granular specimens are nearly saturated, and the liquid bridge is primarily capillary.

However, previous studies mostly operated unilaterally via numerical simulation from macroscopic or mesoscopic perspectives. Under such conditions, the relationship between macroscopic and mesoscopic results is not only hard to correspond, but a corresponding experimental verification is also lacking. As shown in Figure 1, spheres with different radii were selected to eliminate the influence of particle shape on the results. Assuming that water was uniformly distributed in the sphere aggregates, two equal spheres and the liquid bridge between them were regarded as the unit for conducting the mesoscopic experiment.

Using the GCTS testing instrument to measure the SWCCs of the granular specimens composed of particles. Then, a unit body was chosen as an object, the shape parameter of the liquid bridge between two particles was measured with software, and the Young–Laplace (Y–L) equation was used to calculate matric suction between two spheres. The internal mechanism of the influence of particle size on matric suction is analyzed from the perspective of a liquid bridge in a mesoscopic view.

2. Test Procedure

2.1. Test Idea. Spheres with different radii were selected to eliminate the influence of particle shape on the results. Assuming that water was uniformly distributed in the sphere aggregates, two equal spheres and the liquid bridge between them were regarded as the unit for conducting the mesoscopic experiment.

Considering the feasibility of the test operation, the hygroscopicity of the granular specimens composed of large spheres is poor, and thus, small spheres were used. Moreover, the measurement accuracy of Image View software is 0.01 mm, and a large measurement error will be incurred if the particle size is too small. Therefore, large spheres were selected to conduct the mesoscopic experiment.

Although the spheres used in the two tests were of different sizes, the spheres selected in the current study belong to the same scale, and this work only performed qualitative analysis instead of quantitative comparison; thus, the overall design of the test was feasible.

2.2. SWCC Test. The granular specimens were composed of glass spheres with diameters of 0.1, 0.3, and 0.5 mm, respectively. The cylinder specimen was set at 7.1 cm in diameter and 3.19 cm in high, with an initial dry density of 1.58 g/cm^3 . The soil–water characteristic pressure gauge testing system (Figure 2(a)), which was jointly invented by Professor Fredlund and the GCTS company, was used for the SWCC study.

A 5-bar clay plate was first saturated for 3 h and then installed in the instrument base. The filter paper was used to wipe moisture on the surface of the plate, and the cutting ring was placed at the center of the plate. The corresponding quantity of glass beads was weighed, and the beads were poured layer by layer into the cutting ring. The beads were gently compacted to ensure the uniformity of the specimen. The initial water content of the specimen was zero, and thus, the humidification stage was adopted as the initial stage. The infiltration path was set as

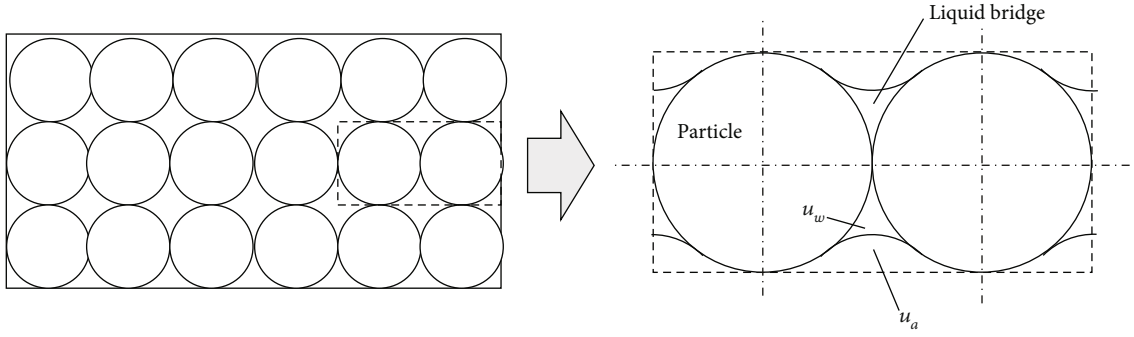


FIGURE 1: Particle aggregate and its unit.

400 kPa → 300 kPa → 200 kPa → 120 kPa → 80 kPa → 50 kPa → 30 kPa → 10 kPa. The reading of the volume tube was recorded after the suction was balanced to calculate the volumetric water content of the specimen. The volume of water content can be obtained by dividing the difference between the readings of the left and right volume tubes by the volume of the particles in the aggregate.

2.3. Liquid Bridge Measurement. Five different volumes (0.1 μL , 0.2 μL , 0.5 μL , 1.0 μL , and 1.5 μL) of a liquid bridge and three kinds of sized spheres (3 mm, 4 mm, and 5 mm in diameter) were selected for tests (Figure 2(b)). Using glycerol instead of water to simulate the liquid bridge between two spheres for its low evaporation and similar surface tension with water, ethyl alcohol, and deionized water were used to remove dust on the surface of the spheres before experiments. The upper sphere was glued to the rigid steel, and the lower sphere was glued to a high-sensitivity spring. A liquid bridge with a known volume was placed on top of the lower spheres by using a microsyringe. The lower sphere was kept immobile while the upper sphere was moved toward the equilibrium position, wherein no deformation occurred in the lower spring. Image View, which is the self-owned numerical measurement software of the CCD camera, was used to measure the neck and outer radii of the liquid bridge. The measurement diagram is shown in Figure 3.

The matric suction of the liquid bridge between two particles can be expressed as Equation (1) in accordance with the Y-L equation.

$$u_a - u_w = \psi = \sigma \left(\frac{1}{r_1} - \frac{1}{r_2} \right). \quad (1)$$

In which ψ is the matric suction, u_a is the air pressure, u_w is the inner pressure of the liquid bridge, σ is the surface tension of the liquid, in this paper it equals 0.068 kN/m, r_1 is the outer radius of the liquid bridge, and r_2 is the neck radius of the liquid bridge, as shown in Figure 3. Substitute the measured results into Equation (1) to obtain the value of matric suction between two spheres.

3. Experiment Results

3.1. SWCC Results. The results of SWCC tests are shown in Figure 4. The SWCCs in this experiment can be divided into

the residual section and transition section. In the residual section, bound water is absorbed onto the surface of a particle. Most pores in the soil are filled with air, and the soil is always dry. In the transition section, the specimen is constantly drained outward, matric suction decreases with an increase in water content, and the unsaturated characteristics start to appear.

The volumetric water content of the granular aggregates exhibited a slow increase followed by a rapid increase with a decrease in matric suction. When matric suction decreased from 400 kPa to 120 kPa, the drainage galleries were discontinuous due to the separation of pore water and pore air, and the volumetric water content increased gradually. When matric suction decreased from 120 kPa to 10 kPa, large amounts of water entered the specimen. At this moment, continuous water films and drainage galleries formed in the specimen, and the volumetric water content increased rapidly. Meanwhile, under the same volumetric water content condition, the specimen composed of larger-sized spheres would gain lower matric suction.

3.2. The SWCCs Obtained by Liquid Bridge Experiment. Taking a microunit body from the sphere aggregate, the pore volume was regarded as the pore between two particles and shown as the light blue area in Figure 5.

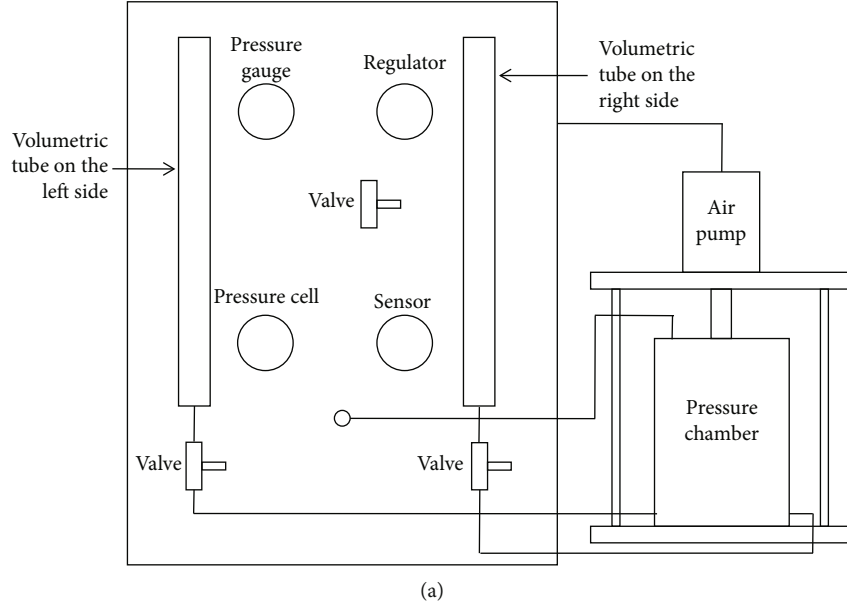
The pore water volume was equal to the volume of the liquid bridge. It is shown as the dark blue area in Figure 5. Then, the saturation of the microunit body can be calculated using the following:

$$S_r = \frac{V_w}{V_v} = \frac{V}{8R^3 - 4/3\pi R^3}. \quad (2)$$

In which S_r is the saturation; V_w is the volume of pore water, μL ; V_v is the pore volume, mm^3 ; V is the volume of the liquid bridge, μL ; and R is the particle radius, mm.

Saturation was converted into the volumetric water content, as shown in Equation (3). The void ratio e can be calculated using Equation (4). For the microunit body in the current study, the void ratio was 0.91.

$$W_V = \frac{S_r}{(1 + 1/e)}, \quad (3)$$



(b)

FIGURE 2: Testing instruments. (a) The GCTS soil–water characteristic pressure gauge testing instrument was used to test the SWCCs of the granular specimens. (b) The liquid bridge tension instrument.

$$e = \frac{V_v}{V_s} = \frac{8R^3 - 4/3\pi R^3}{4/3\pi R^3} = 0.91. \quad (4)$$

The outer radius of the liquid bridge on the left and right sides was measured. The left side outer radius was denoted as $r_{1\text{left}}$ and the right side outer radius was denoted as $r_{1\text{right}}$. The average of $r_{1\text{left}}$ and $r_{1\text{right}}$ was considered the

final outer radius and denoted as $r_{1\text{equal}}$. The value of matric suction can be obtained by substituting the surface tension of glycerol, r_2 and $r_{1\text{equal}}$ into Equation (1). The results are presented in Table 1.

To make a direct comparison with the results in Section 3.1, setting matric suction as the horizontal axis and volumetric water content as the vertical axis. The relationship

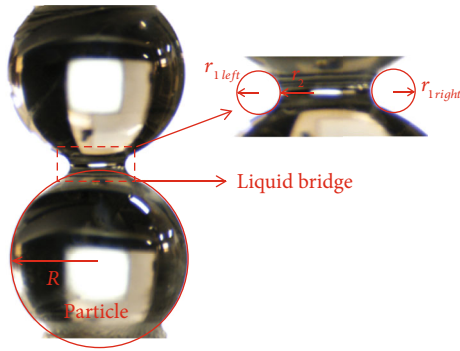


FIGURE 3: Measuring the geometric parameter of the liquid bridge through Image View software.

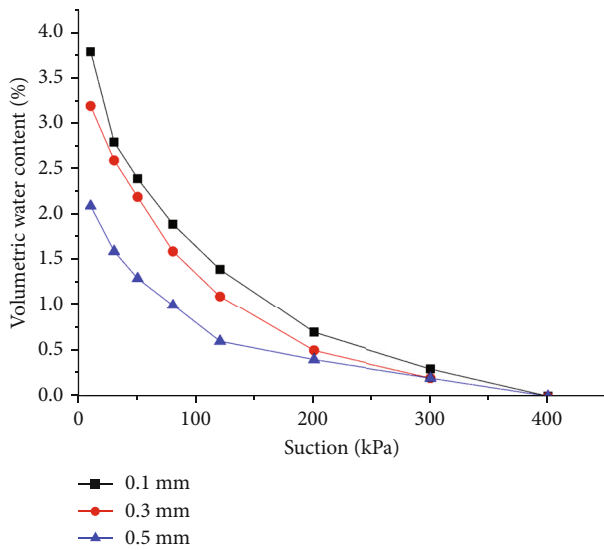


FIGURE 4: SWCCs for specimens composed of different-sized spheres.

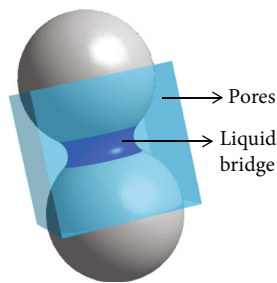


FIGURE 5: Calculation diagram of saturation between two spheres.

between volumetric water content and matric suction in Table 1 is illustrated in Figure 6.

As shown in Figure 6, for the SWCCs obtained from the liquid bridge experiment, matric suction also experienced a rapid to slow increase with a decrease in volumetric water content. When volumetric water content changed from 10% to 0.4%, matric suction achieved a high increase rate.

When volumetric water content changed from 0.3% to 0.1%, the increase in matric suction slowed down. Meanwhile, when the volumetric water content was equal, the smaller the sphere radius, the higher the matric suction between the two spheres. This finding is consistent with the macroscopic SWCC results.

When $D = 3 \text{ mm}$ $V = 1.5 \mu\text{L}$, the profile of the liquid bridge was convex, shown in Figure 7. The value of r_1 cannot be measured, which means that the Y-L equation in an unsaturated soil field is no longer suitable under this condition.

4. Discussion

The Y-L equation is unsuitable under the condition in which $D = 3 \text{ mm}$ $V = 1.5 \mu\text{L}$. Therefore, the application scope of liquid bridge theory used to identify the internal change mechanism of SWCCs must be determined.

In accordance with previous research, the liquid bridge profile is largely determined by gravity. Kazuyuki et al. [25] introduced the concept of the Bo number by studying the relationship between liquid volume and gravity. The product of the dimensionless volume V^* and the Bo number is used to reflect the influence of gravity on the liquid bridge profile between two spheres. When $V^* \cdot Bo < 0.01$, the effect of gravity can be disregarded. When $V^* \cdot Bo > 0.15$, the effect of gravity cannot be disregarded. When $0.01 < V^* \cdot Bo < 0.15$, the effect of gravity is in the transition stage [26]. The dimensionless liquid volume and the Bo number can be calculated using Equations (5) and (6), respectively.

$$V^* = \frac{V}{R^3}, \tag{5}$$

$$Bo = \frac{\Delta\rho g d^2}{\sigma}. \tag{6}$$

In which $\Delta\rho$ is the density difference between liquid and the external air, kg/m^3 ; g is the gravitational acceleration, m/s^2 ; and d is the characteristic length, which is a function of the liquid volume, as Equation (7) shows.

$$d = \sqrt{\frac{V}{D}}. \tag{7}$$

In which D is the diameter of the sphere and V has the same meaning as mentioned above.

In this article, $\Delta\rho = 1260 \text{ kg/m}^3$, $\sigma = 0.068 \text{ N/m}$, and $g = 9.81 \text{ m/s}^2$, and $D = 3 \text{ mm}$, 4 mm , and 5 mm , respectively. By substituting these values into Equations (5) and (6), the calculated results and the influence of gravity are presented in Table 2.

As indicated in Tables 1 and 2, the cases in which liquid bridge theory is applicable are all under the condition wherein the effect of gravity can be disregarded, the profile of the liquid bridge in this stage is concave, and the theory can identify the internal change mechanism of SWCCs. When the influence of gravity is in the transition stage, the liquid bridge theory still makes sense; however, the profile of a liquid bridge is nonaxisymmetrically concave, and a

TABLE 1: The measured and calculated results for the equal sphere system.

Diameter/ mm	Liquid volume/ μL	Pore volume/ mm^3	Saturation/ %	Volumetric water content/%	$r_{1\text{left}}/\text{mm}$	$r_{1\text{right}}/\text{mm}$	$r_{1\text{equal}}/\text{mm}$	r_2/mm	Ψ/pa
3	0.1	4.09	2.44	1.16	0.33	0.34	0.34	0.58	76.67
	0.2		4.89	2.33	0.43	0.43	0.43	0.75	61.37
	0.5		12.22	5.82	0.52	0.51	0.52	0.77	39.34
	1		24.45	11.65	0.61	0.68	0.65	0.79	17.17
	1.5		36.67	17.47					
4	0.1	16.76	0.60	0.29	0.35	0.33	0.34	0.73	98.99
	0.2		1.19	0.57	0.42	0.42	0.42	0.85	75.88
	0.5		2.99	1.42	0.52	0.50	0.51	0.97	58.58
	1		5.97	2.84	0.66	0.60	0.63	1.02	38.24
	1.5		8.96	4.27	0.63	0.77	0.70	1.05	36.75
5	0.1	32.72	0.31	0.15	0.35	0.35	0.35	0.78	99.23
	0.2		0.61	0.29	0.41	0.43	0.42	0.88	78.41
	0.5		1.53	0.73	0.50	0.48	0.49	0.99	64.94
	1		3.06	1.46	0.59	0.62	0.61	1.08	44.95
	1.5		4.58	2.18	0.64	0.70	0.67	1.12	37.78

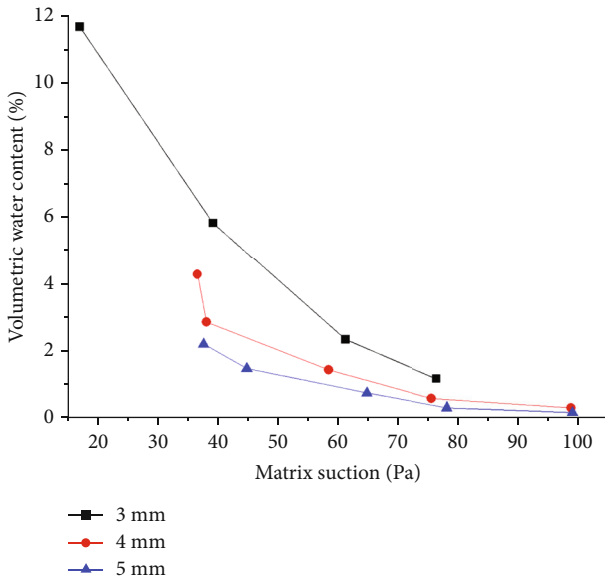


FIGURE 6: The SWCCs obtained by liquid bridge experiment.

difference exists between $r_{1\text{left}}$ and $r_{1\text{right}}$. When the influence of gravity cannot be disregarded ($D = 3 \text{ mm}$, $V = 1.5 \mu\text{L}$), the profile of a liquid bridge is convex, and liquid bridge theory is unsuitable. According to the saturation degree and inner mechanism of the liquid bridge, the liquid bridge within particles can be divided into pendular, funicular, capillary, and slurry states, shown as Table 3.

Therefore, identifying the internal change mechanism of SWCCs from the perspective of a liquid bridge is only applicable when the liquid volume is small, the influence of gravity can be disregarded or is in the transitional stage, and the profile of a liquid bridge is concave. If the liquid bridge volume is greater than the volume required to form a concave



FIGURE 7: Profile of liquid bridge when the Y-L equation is not suitable.

bridge, then the bridge adopts a cylindrical or convex shape, and liquid bridge theory is no longer applicable.

The relationship between volumetric water content and r_1 and r_2 is illustrated in Figure 8. Both r_1 and r_2 increase with the increase of volumetric water content, r_1 shows a continuously increasing trend while r_2 increases first and then maintains stable. The inflection point of the volumetric water content- r_2 curve increases with the addition of sphere diameter, under the condition of $D = 3 \text{ mm}$, the inflection point corresponds to about 2.2% of the volumetric water content. Under the condition of $D = 4 \text{ mm}$, although there is no obvious

TABLE 2: The Bo number and effects of gravity.

D/mm	$V/\mu L$	V^*	d^2/mm^2	Bo	$V^* \cdot Bo$	Gravity effect
3	0.1	0.051	0.08	0.015	7.5×10^{-4}	No
	0.25	0.128	0.20	0.037	0.005	No
	0.5	0.256	0.40	0.074	0.019	Transition
	1.0	0.512	0.80	0.148	0.076	Transition
	1.5	0.768	1.20	0.221	0.170	Yes
4	0.1	0.013	0.05	0.009	1.1×10^{-4}	No
	0.25	0.031	0.13	0.024	7.4×10^{-4}	No
	0.5	0.063	0.25	0.046	0.003	No
	1.0	0.125	0.50	0.092	0.012	Transition
	1.5	0.188	0.75	0.138	0.026	Transition
5	0.1	0.006	0.04	0.007	4.4×10^{-5}	No
	0.25	0.016	0.10	0.018	2.9×10^{-4}	No
	0.5	0.032	0.20	0.037	0.001	No
	1.0	0.064	0.40	0.074	0.005	No
	1.5	0.096	0.60	0.111	0.011	Transition

TABLE 3: Classification of the liquid bridge.

Pendular	$0\% < Sr < 30\%$	Liquid bridge formed at the contact point of particles
Funicular	$30\% < Sr < 70\%$	Liquid bridge filled with part of the particle gap, there exist few saturated parts in the specimen
Capillary	$70\% < Sr < 100\%$	Almost all pores in the specimen are filled with liquid
Slurry	$Sr > 100\%$	All pores in the specimen are filled with liquid; the liquid pressure is greater than the air pressure

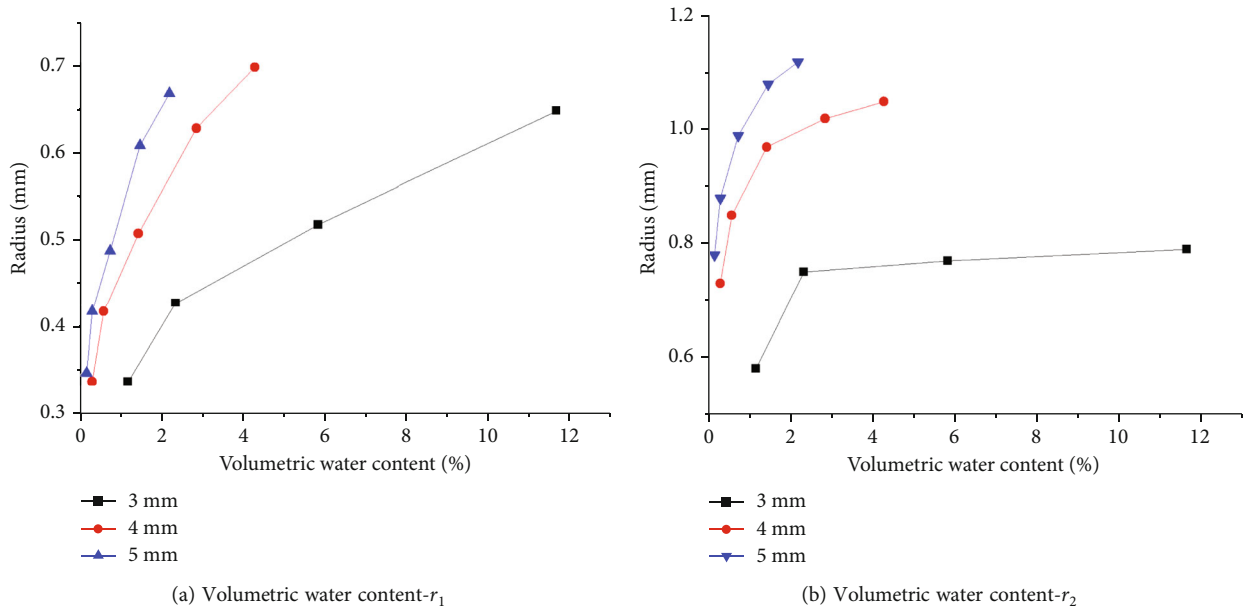


FIGURE 8: The relationship between the volumetric water content and r_1 and r_2 .

inflection point, the growth rate has slowed down. Under the condition of $D = 5$ mm, the deceleration trend is not obvious.

On the one hand, although the value of r_1 is always smaller than r_2 , the increasing rate of r_1 is significantly higher than r_2 when the volumetric water content varies in

the same range. For spheres of $D = 4$ mm, r_1 increased by 97% and r_2 increased by 51% when the volumetric water content increased from 0.29% to 4.27%. For spheres of $D = 5$ mm, r_1 increased by 91% and r_2 increased by 43% when the volumetric water content increased from 0.15% to 2.18%. On the other hand, for the larger diameter of spheres, the curves of volumetric water content- r_1 and r_2 gain a steeper slope, which means a higher increasing rate of r_1 and r_2 will gain.

It can be inferred that the influence of sphere radius on matric suction is mostly caused by the variation in r_1 and r_2 . On the one hand, with an increase in volumetric water content, the pore pressure (atmospheric pressure) remains stable. Under the action of pore water pressure, the liquid bridge continuously extends outward, leading to the increase of r_1 and r_2 , while in this progress, the increasing rate of r_1 is much higher than r_2 . On the other hand, when the liquid volume equals, for small-sized spheres, the liquid-solid interface corresponding is limited. The liquid-solid interface increases with the increase in diameter; the liquid bridge can be better spread out, while in this progress, the sensitivity of r_1 to the diameter of the sphere is much higher than r_2 . These all lead to the decreases of difference between the reciprocal of r_1 and that of r_2 , and the macroscopical matric suction gradually decreases.

5. Conclusions

This study selected granular specimen as research object and used a GCTS testing instrument to measure the SWCCs of the specimens, which were composed of spheres with diameters of 0.1, 0.3, and 0.5 mm, respectively, to study water retention properties from the macroscopic perspective. Two equal spheres with three different sizes (3 mm, 4 mm, and 5 mm in diameter) and the liquid bridge between them with five different volumes (0.1, 0.2, 0.5, 1.0, and 1.5 μL) were regarded as the unit body to study water retention properties from the mesoscopic perspective. The matric suction between the two spheres was obtained by measuring the shape parameter of the unit body and using the Y-L equation. The internal mechanism of the influence of volumetric water content and particle size on matric suction was analyzed from the macroscopic and mesoscopic perspectives. Meanwhile, the application scope of liquid bridge theory, which was used to identify the internal change mechanism of SWCCs, was discussed. Finding that:

- (1) The mesoscopic experiments showed that the smaller the sphere radius, the higher the matric suction between two spheres. This finding is consistent with the macroscopic SWCC results
- (2) Identifying the internal change mechanism of SWCCs from a liquid bridge perspective is only applicable when the influence of gravity can be disregarded or in the transitional stage and the profile of the liquid bridge is concave. If the influence of gravity cannot be disregarded, the liquid bridge adopts a

convex shape, then the liquid bridge theory is no longer applicable

- (3) The influence of volumetric water content and sphere radius on matric suction is mostly caused by the variation in r_1 and r_2 . With an increase in volumetric water content and sphere diameter, the increasing rate of r_1 is much higher than r_2 . The liquid-solid interface increases with the increase in diameter, while in this progress, the sensitivity of r_1 to the diameter of the sphere is much higher than r_2 . These both lead to decreases in the difference between the reciprocal of r_1 and that of r_2 , and the macroscopical matric suction gradually decreases

Data Availability

The data used to support the findings of this study are included within the article.

Conflicts of Interest

The authors declare that they have no conflicts of interest.

Acknowledgments

This study was funded by the National Natural Science Foundation of China (nos. 51679198 and 12072260).

References

- [1] M. Y. Fattah, N. M. Salim, and E. J. Irshayyid, "Determination of the soil-water characteristic curve of unsaturated bentonite-sand mixtures," *Environmental Earth Sciences*, vol. 76, no. 5, pp. 1–12, 2017.
- [2] M. Y. Fattah, A. A. H. Al-Obaidi, and M. K. Al-Dorry, "Determination of the soil water characteristic curve for unsaturated gypseous soil from model tests," *Research Journal of Applied Sciences*, vol. 13, no. 9, pp. 544–551, 2019.
- [3] S. K. Vanapalli, D. G. Fredlund, and D. E. Pufahl, "The relationship between the soil-water characteristic curve and the unsaturated shear strength of a compacted glacial till," *Geotechnical Testing Journal*, vol. 19, no. 3, pp. 259–268, 1996.
- [4] D. G. Fredlund, D. Sheng, and J. Zhao, "Estimation of soil suction from the soil-water characteristic curve," *Canadian Geotechnical Journal*, vol. 48, no. 2, pp. 186–198, 2011.
- [5] C. L. Chen, F. Chu, L. L. Li, and Z. M. Cao, "Soil-water characteristics of unsaturated undisturbed loess under confined compression condition," *Chinese Journal of Rock Mechanics and Engineering*, vol. 30, no. 3, pp. 610–615, 2011.
- [6] C. Malaya and S. Sreedeeep, "Critical review on the parameters influencing soil-water characteristic curve," *Journal of Irrigation and Drainage Engineering*, vol. 138, no. 1, pp. 55–62, 2012.
- [7] M. S. R. Buisson, S. J. Wheeler, and R. S. Sharma, "Coupling of hydraulic hysteresis and stress-strain behaviour in unsaturated soils," *Géotechnique*, vol. 53, no. 1, pp. 41–54, 2003.
- [8] R. A. Fisher, "On the capillary forces in an ideal soil; correction of formulae given by W. B. Haines," *Journal of Agricultural Science*, vol. 16, no. 3, pp. 492–505, 1926.
- [9] T. Gillespie and W. J. Settineri, "The effect of capillary liquid on the force of adhesion between spherical solid particles,"

- Journal of Colloid and Interface Science*, vol. 24, no. 2, pp. 199–202, 1967.
- [10] W. C. Clark, J. M. Haynes, and G. Mason, “Liquid bridges between a sphere and a plane,” *Chemical Engineering Science*, vol. 23, no. 7, pp. 810–812, 1968.
- [11] Z. Fournier, D. Geromichalos, S. Herminghaus et al., “Mechanical properties of wet granular materials,” *Journal of Physics*, vol. 17, no. 9, pp. S477–S502, 2005.
- [12] D. Rossetti and S. J. R. Simons, “A microscale investigation of liquid bridges in the spherical agglomeration process,” *Powder Technology*, vol. 130, no. 1-3, pp. 49–55, 2003.
- [13] K. N. Manahiloh, B. Muhunthan, and W. J. Likos, “Microstructure-based effective stress formulation for unsaturated granular soils,” *International Journal of Geomechanics*, vol. 16, no. 6, 2016.
- [14] F. Molenkamp and A. H. Nazemi, “Interactions between two rough spheres, water bridge and water vapour,” *Géotechnique*, vol. 53, no. 2, pp. 255–264, 2003.
- [15] W. J. Likos and N. Lu, “Hysteresis of capillary stress in unsaturated granular soil,” *Journal of Engineering Mechanics*, vol. 130, no. 6, pp. 646–655, 2004.
- [16] X. L. Jiang and P. C. Li, “Calculation of intergranular suction considering cementing area between soil particles,” *Chinese Journal of Geotechnical Engineering*, vol. 38, no. 6, pp. 1160–1164, 2016.
- [17] F. Soulié, F. Cherblanc, M. S. El Youssoufi, and C. Saix, “Influence of liquid bridges on the mechanical behaviour of polydisperse granular materials,” *International Journal for Numerical and Analytical Methods in Geomechanics*, vol. 30, no. 3, pp. 213–228, 2006.
- [18] S. Yang and T. H. Lu, “Study of soil-water characteristic curve using microscopic spherical particle model,” *Pedosphere*, vol. 22, no. 1, pp. 103–111, 2012.
- [19] G. C. Cho and J. C. Santamarina, “Unsaturated particulate materials - particle-level studies,” *Journal of Geotechnical and Geoenvironmental Engineering*, vol. 127, no. 1, pp. 84–96, 2001.
- [20] L. Scholtes, B. Chareyre, F. Nicot, and F. Darve, “Micromechanics of granular materials with capillary effects,” *Internal Journal of Engineering Science*, vol. 47, no. 1, pp. 64–75, 2009.
- [21] D. G. Fredlund and A. Xing, “Equations for the soil-water characteristic curve,” *Canadian Geotechnical Journal*, vol. 31, no. 4, pp. 521–532, 1994.
- [22] I. A. Abd, M. Y. Fattah, and H. Mekkiyah, “Relationship between the matric suction and the shear strength in unsaturated soil,” *Construction Materials*, vol. 13, article e00441, 2020.
- [23] F. Gabrieli, P. Lambert, S. Cola, and F. Calvetti, “Micromechanical modelling of erosion due to evaporation in a partially wet granular slope,” *International Journal for Numerical and Analytical Methods in Geomechanics*, vol. 36, no. 7, pp. 918–943, 2012.
- [24] D. Fredlund, “Unsaturated soil mechanics in engineering practice,” *Journal of Geotechnical and Geoenvironmental Engineering*, vol. 132, no. 3, pp. 286–321, 2006.
- [25] H. Kazuyuki, T. Kazuo, and I. Koichi, “The capillary binding force of a liquid bridge,” *Powder Technology*, vol. 10, no. 4-5, pp. 231–242, 1974.
- [26] M. J. Adams, S. A. Johnson, J. P. K. Seville, and C. D. Willett, “Mapping the influence of gravity on pendular liquid bridges between rigid spheres,” *Langmuir*, vol. 18, no. 16, pp. 6180–6184, 2002.